



HAL
open science

Crystal structure refinement and electronic properties of Si(cI16)

Aron Wosylus, Helge Rosner, Walter Schnelle, Ulrich Schwarz

► **To cite this version:**

Aron Wosylus, Helge Rosner, Walter Schnelle, Ulrich Schwarz. Crystal structure refinement and electronic properties of Si(cI16). *Journal of Inorganic and General Chemistry / Zeitschrift für anorganische und allgemeine Chemie*, 2009, 635 (4-5), pp.700. 10.1002/zaac.200900051 . hal-00482072

HAL Id: hal-00482072

<https://hal.science/hal-00482072>

Submitted on 8 May 2010

HAL is a multi-disciplinary open access archive for the deposit and dissemination of scientific research documents, whether they are published or not. The documents may come from teaching and research institutions in France or abroad, or from public or private research centers.

L'archive ouverte pluridisciplinaire **HAL**, est destinée au dépôt et à la diffusion de documents scientifiques de niveau recherche, publiés ou non, émanant des établissements d'enseignement et de recherche français ou étrangers, des laboratoires publics ou privés.



Crystal structure refinement and electronic properties of Si(cI16)

Journal:	<i>Zeitschrift für Anorganische und Allgemeine Chemie</i>
Manuscript ID:	zaac.200900051
Wiley - Manuscript type:	Article
Date Submitted by the Author:	19-Jan-2009
Complete List of Authors:	Wosylus, Aron; MPI CPfS, Chemische Metallkunde Rosner, Helge; MPI CPfS, Chemische Metallkunde Schnelle, Walter; MPI CPfS, Chemische Metallkunde Schwarz, Ulrich; MPI CPfS, Chemische Metallkunde
Keywords:	Silicon, Allotropy, Crystal Structure, Electronic Density of States, Physical Properties



Crystal structure refinement and electronic properties of Si(*cI16*)

Aron Wosylus, Helge Rosner, Walter Schnelle, Ulrich Schwarz*

Max-Planck-Institut für Chemische Physik fester Stoffe, Dresden

Dedicated to Prof. Reinhard Nesper on the occasion of his 60th birthday

Abstract. Si(*cI16*) is prepared in polycrystalline form at 12(1.5) GPa at temperatures between 800(80) K and 1200(120) K. The crystal structure is refined by a full-profile method using x-ray powder diffraction data. Si(*cI16*) is diamagnetic ($\chi_0 = -5.6(1.8) \times 10^{-6}$ emu mol⁻¹) and shows a weakly temperature-dependent electrical resistivity ($\rho(300\text{ K}) = 0.3 \times 10^{-3}$ Ω m). Computations of structural and electronic properties of Si(*cI16*) within the local density approximation evidence the metastable character of the allotrope with respect to diamond-type silicon. The calculations yield a positional parameter which is in perfect agreement with the refined value. In agreement with the experimentally observed conductivity properties, the computed density of states evidence that the Fermi level of Si(*cI16*) is located in a pseudo-gap.

Keywords: Silicon; Allotropy; Crystal Structure; Electronic Density of States; Physical Properties

*PD Dr. U. Schwarz

Max-Planck-Institut für Chemische Physik fester Stoffe

Nöthnitzer Straße 40, 01187 Dresden, Germany

Fax: (+49) 351-4646-4002

E-mail: schwarz@cpfs.mpg.de

Introduction

In the course of investigations on binary tetrels of alkaline-earth metals manufactured at high-pressure high-temperature conditions [1–4], we observed the metastable element modifications Ge(*tP12*) [5, 6] and Si(*cI16*) [7] as minority phases after application of pressures slightly above ten GPa with a large-volume two-stage multi-anvil device. Si(*cI16*) was described for the first time more than forty years ago. The crystal structure (Fig. 1) was solved on the basis of x-ray powder diffraction data, but the position parameter of silicon was only estimated by visual comparison of experimental and calculated x-ray diffraction intensities. In the atomic arrangement which is isotopic to Ge(*cI16*) [8], four-coordinated silicon atoms are reported to adopt a trigonal pyramidal coordination with $d(\text{Si-Si})$ of $1 \times 2.369(9)$ Å and $3 \times 2.384(9)$ Å [7] instead of tetrahedral with $d(\text{Si-Si}) = 2.351$ Å [9] in ambient pressure Si(*cF8*).

Later in-situ investigations at high pressures [10] including studies of the formation of Si(*cI16*) at elevated temperatures [11, 4] as well as determinations of the electrical resistance were performed on minute samples using the diamond anvil cell technique [12]. The results evidence that, at ambient temperature, the phase Si(*cI16*) is metastable between ambient pressure and at least 2 GPa. Transformation at normal pressure requires heating to 423 K for several hours [7].

The renewed interest in crystal structure and physical properties of Si(*cI16*) is motivated by the lack of magnetic measurements and refined structural data as well as by the importance of the allotrope as a prototype tetrahedral framework with a differentiation of interatomic distances due to a decrease of symmetry. We report here the least squares refinement of crystal structure parameters using x-ray powder diffraction data and measurements of magnetic properties and electrical transport features. Concomitant band structure calculations independently evaluate the stability of the allotrope and the refined structural parameter. Moreover, they shed light on the electronic structure and the specific changes caused by the deviation of the coordination polyhedron from tetrahedral symmetry.

Experiments and band structure calculations

Si(*cI16*) was synthesized from the starting material Si(*cF8*) (Alpha Aesar 99.9999 %) at 12(1.5) GPa and temperatures between 800(100) K and 1200(120) K in a hydraulic press equipped with a Walker-type module [13, 14]. Typically, pressure was increased within 4 h and released within 10 h. Pressure calibration had been performed prior to the experiments measuring the resistance changes associated with the phase transitions of Bi [15] and Pb [16–18]. The temperature-current relation had been determined in separate runs with W/WRe thermocouples. Heating was realized with graphite tubes. Hexagonal boron nitride served as crucible material. No apparent reaction with silicon at the selected transformation conditions was observed. X-ray powder diffraction experiments were performed in transmission arrangements (Huber Image Plate G670 with $\text{Cu}_{\text{K}\alpha 1}$ radiation and at ID31 of the ESRF using a high-resolution set-up and synchrotron radiation). Details concerning measurement and refinement as well as selected results are given in Tab. 1.

The samples for the physical measurements on Si(*cI16*) were two polycrystalline pieces from separate high-pressure synthesis runs. The magnetization was determined in magnetic fields $\mu_0 H = 3.5$ T and 7 T between 1.8 K and 300 K and also at lower fields in a SQUID magnetometer (MPMS XL-7, Quantum Design). The sample

1
2
3 consisted of 2 pieces with a total mass of 27.82 mg co-mounted with GE-7031 varnish to a thin quartz rod.
4 Corrections for the sample holder and the glue were applied. The electrical resistance was measured by a linear
5 four-point method using alternating current in the temperature range 1.8 – 380 K. For that purpose one piece was
6 ground to dimensions $1.85 \times 1.90 \times 1.14 \text{ mm}^3$. Due to the uncertainties of the contact distance and the cross-
7 section the estimated inaccuracy of the electrical resistivity is $\pm 30 \%$. For comparison the resistivity data of
8 another piece (dc measurement, 4 – 320 K) are given.

9
10 For electronic structure calculations the full-potential local-orbital scheme FPLO (version: FPLO 8.00-31) within
11 the local density approximation (LDA) was used [19]. In the scalar relativistic calculations the exchange and
12 correlation potential of Perdew and Wang was chosen [20]. To ensure accurate total energy and density of states
13 (DOS) information, a fine, well converged k -mesh of 9486 points in the irreducible part of the Brillouin zone
14 was used.

21 Results and Discussion

22
23 Within the investigated pressure and temperature range, syntheses yields polycrystalline single-phase Si(*cI16*) in
24 all experiments. X-ray powder diffraction patterns (Fig. 2) reveal a significant peak broadening, e.g., for the
25 strongest reflection (121) a full width at half maximum of 0.08° at $2\theta = 8.477^\circ$. By applying the *Scherrer*-
26 equation [21] this corresponds to an average domain size of roughly 250 Å. The small particle dimension is
27 attributed to a first-order transition of the intermediate high-pressure phase Si(*hR8*) into Si(*cI16*) at pressures
28 around 2 GPa [10] upon decompression.

29
30 The structure model of the earlier solution is refined by means of a least squares procedure using complete x-ray
31 powder diffraction diagrams (Fig. 2). The supposed atomic arrangement [7] is essentially confirmed by the
32 results with the main exception that the present analysis of the high-quality synchrotron x-ray diffraction
33 intensities evidences a difference of the crystallographically independent interatomic distances of about 0.06 Å
34 (see Tab. 1). Thus, Si(*cI16*) belongs indeed to the small, but still growing set of high-pressure phases in which
35 the reduction of point symmetry is associated with a differentiation of chemically equivalent interatomic
36 distances [22].

37
38 The high-field magnetic susceptibility $\chi(T) = M/H$ (Fig. 3, top) of the sample is slightly dependent on field,
39 which indicates minor ferromagnetic impurities. The latter are taken into account by the Honda-Owen
40 extrapolation for each temperature. The weakly temperature-dependent correction applied to the 7 T data
41 corresponds to approximately $-1.5 \times 10^{-6} \text{ emu mol}^{-1}$, which would be consistent with, e.g., a mass content of
42 elemental Fe of 16×10^{-6} . The resulting susceptibility still displays a weak Curie contribution. The intrinsic,
43 essentially temperature-independent susceptibility of Si (*cI16*) is obtained by a fit: $\chi_0(T = 0 \text{ K}) = -5.6(1.8) \cdot 10^{-6}$
44 emu mol^{-1} , the value of $\chi(300 \text{ K})$ is $-5.3(1.5) \cdot 10^{-6} \text{ emu mol}^{-1}$. For comparison, the value of $\chi(300 \text{ K})$ for
45 Si(*cF8*) is $-3.12 \cdot 10^{-6} \text{ emu mol}^{-1}$ [23] or, according to a different source, $-5.3 \cdot 10^{-6} \text{ emu mol}^{-1}$ [24]. No phase
46 transitions are observed in the covered temperature range.

47
48 The temperature dependence of the electrical resistivity (Fig. 3, bottom) is rather weak: from a room-temperature
49 value $\rho(300 \text{ K}) = 0.3 \cdot 10^{-3} \Omega \text{ m}$ the resistivity increases only to $\rho_0 = 1.0 \cdot 10^{-3} \Omega \text{ m}$ at 1.8 K. The value at 100 K
50 of $0.6 \cdot 10^{-3} \Omega \text{ m}$ compares very well with that in a previous investigation ($\rho(100 \text{ K}) = 0.5 \cdot 10^{-3} \Omega \text{ m}$ [12]). In
51 order to check the variation among different samples and primings, we measured a second piece from another
52 synthesis run (see Fig. 3b). The resistivity is slightly higher but shows almost the same temperature dependence.

1
2
3 For $T > 50$ K and at least up to 350 K the conductivity $\sigma(T)$ of our Si(*cI16*) samples increases linearly with
4 temperature. The same observation for $\sigma(T)$ has been previously attributed to localization effects in a disordered
5 system [12]. Below 10 K, the equation $\sigma(T) = \sigma_0 + aT^\alpha$ with $\alpha = 3/2$ can be well fitted to the recent conductivity
6 measurements while in an analysis of earlier data a power law with $\alpha = 2$ has been applied [12].
7

8
9 As an independent approach to both the electronic and the structural features of metastable Si(*cI16*), we applied
10 a highly accurate full-potential band structure scheme to calculate electronic structure and total energies for
11 Si(*cI16*). As a reference, well-known diamond-type Si(*cF8*) is selected. For the experimentally determined
12 lattice parameters at ambient conditions, diamond-type silicon is more stable than the metastable cubic allotrope
13 by an energy difference of about 130 meV per atom (12.6 kJ/mol). For the same unit cell volume, the positional
14 parameter x for Si(*cI16*) was optimized (Fig. 4). The equilibrium position is calculated to $x_{\text{theo}} = 0.10149(5)$ in
15 excellent agreement with the experimental value $x_{\text{exp}} = 0.10143(4)$ (see Tab. 1 and comment therein).
16

17 Figure 5 shows a comparison of the calculated electronic DOS of Si(*cI16*) and Si(*cF8*). We find semiconducting
18 behaviour for the diamond-type phase of silicon with a DOS gap of about 0.5 eV. The underestimation with
19 respect to the experimental value of about 1.1 eV is related to the well-known gap problem of the LDA. In
20 contrast, for Si(*cI16*) we find that the Fermi level ε_F is located in a pronounced pseudo-gap with a low density of
21 states. A corresponding calculation for a model with equidistant neighbours provides rather large values for the
22 DOS at ε_F . Thus, the emergence of the local DOS minimum for Si(*cI16*) is clearly caused by the differentiation of
23 the distances $d(\text{Si-Si})$ within the trigonal pyramidal coordination.
24

25 The valence band width of Si(*cI16*) is slightly larger (about 1 eV) than that of Si(*cF8*). A model with four
26 equivalent distances $d(\text{Si-Si})$ and an additional adjustment of the interatomic distances to the value of diamond-
27 type silicon yields a valence band width which is very close to that of Si(*cF8*). This finding reveals that the
28 slightly larger valence band width of Si(*cI16*) compared to diamond-type silicon is mainly caused by the shorter
29 next-neighbour distance.
30

31 As a summary, we have collected additional theoretical and experimental evidence for the difference of the
32 symmetry-independent interatomic distances in the trigonal pyramidal coordination sphere of silicon atoms in
33 Si(*cI16*). In accordance with the findings of resistivity measurements, band structure calculations reveal
34 substantial differences of the electronic features which can be traced back to the dissimilarity of the atomic
35 arrangements of Si(*cF8*) and Si(*cI16*). The results concerning total energy and atomic position establish
36 elaborate band structure calculations once more as a valuable and reliable tool for gaining deeper insight into
37 crystal structure properties and phase diagrams of elements [25, 26].
38

39 40 41 42 43 44 45 46 47 48 49 50 51 **Acknowledgement**

52
53
54 For supporting high-pressure synthesis we thank Carola J. Müller, Susann Leipe and Knut Range. Help with the
55 high-resolution x-ray powder diffraction measurements by Irene Margiolaki at the ESRF is gratefully
56 acknowledged. Special thanks to Ralf Koban for fastidious sample priming.
57
58
59
60

References

- [1] A. Wosylus, Yu. Prots, U. Burkhardt, W. Schnelle, U. Schwarz, Yu. Grin, *Solid State Sci.* **2006**, *8*, 773.
- [2] A. Wosylus, Yu. Prots, U. Burkhardt, W. Schnelle, U. Schwarz, Yu. Grin, *Z. Naturforschung, B* **2006**, *61*, 1485.
- [3] A. Wosylus, Yu. Prots, U. Burkhardt, W. Schnelle, U. Schwarz, *Sci. Technol. Adv. Mater.* **2007**, *8*, 383.
- [4] A. Wosylus, PhD Thesis, University of Dresden, submitted.
- [5] F. P. Bundy, J. S. Kasper, *Science* **1963**, *139*, 340.
- [6] A. Wosylus, Yu. Prots, W. Schnelle, U. Schwarz, *Z. Naturforschung, B* **2008**, *63*, 608.
- [7] R.H. Wentorf Jr., J.S. Kasper, *Science* **1963**, *139*, 338.
- [8] R. J. Nelmes, M. I. McMahon, N. G. Wright, D. R. Allan, J. S. Loveday, *Phys. Rev. B* **1993**, *48*, 9883.
- [9] R.R. Reeber and B.A. Kulp, *Trans. Met. Soc. AIME* **1965**, *233*, 698.
- [10] J. Crain, G.J. Ackerland, J.R. Maclean, R.O. Piltz, P.D. Hatton, G.S. Pawley, *Phys. Rev. B* **1994**, *50*, 13043.
- [11] G. Weill, J. L. Mansot, G. Sagon, C. Carlone, J. M. Besson, *Semicond. Sci. Technol.* **1989**, *4*, 280.
- [12] J.M. Besson, E.H. Mokhtari, J. Gonzalez, G. Weill, *Phys. Rev. Lett.* **1987**, *59*, 473.
- [13] D. Walker, M.A. Carpenter, C.M. Hitch, *Am. Mineral.* **1990**, *75*, 1020.
- [14] H. Huppertz, *Z. Kristallogr.* **2004**, *219*, 330.
- [15] I. C. Getting, *Metrologia* **1998**, *35*, 119.
- [16] T. Takahashi, H. Kwang, W.A. Bassett, *Science* **1969**, *165*, 1352.
- [17] L.F. Vereshchagin, A.A. Semerchan, N.N. Kuzin, Y.A. Sadkov, *Sov. Phys. Dokl.* **1970**, *15*, 295.
- [18] H. Mii, I. Fujishiro, M. Senoo, K. Okawa, *High Temp.-High Pressures* **1973**, *5*, 155.
- [19] K. Koepernik, and H. Eschrig, *Phys. Rev. B* **1999**, *59*, 1743.
- [20] J.P. Perdew and Y. Wang, *Phys. Rev. B* **1992**, *45*, 13244.
- [21] P. Scherrer, *Nachr. Ges. Wiss. Göttingen* **1918**, 100.
- [22] R. Demchyna, S. Leoni, H. Rosner, U. Schwarz, *Z. Kristallogr.* **2006**, *221*, 420.
- [23] CRC Handbook of Chemistry and Physics, 87th ed., D. R. Lide (Ed.), CRC Press, Boca-Raton **2007**.
- [24] P. W. Selwood, *Magnetochemistry*, 2nd ed., Interscience, New York **1956**.
- [25] U. Schwarz, L. Akselrud, H. Rosner, A. Ormeci, Yu. Grin, M. Hanfland, *Phys. Rev. B* **2003**, *67*, 214101.
- [26] A. Ormeci, K. Koepernik, and H. Rosner, *Phys. Rev. B* **2006**, *74*, 104119.
- [27] L.G. Akselrud, P.Yu. Zavalii, Yu. Grin, V.K. Pecharski, B. Baumgartner, E. Wölfel, *Mater. Sci. Forum* **1993**, 133.
- [28] J. Rodriguez-Carvajal, *Physica B* **1993**, *192*, 55.

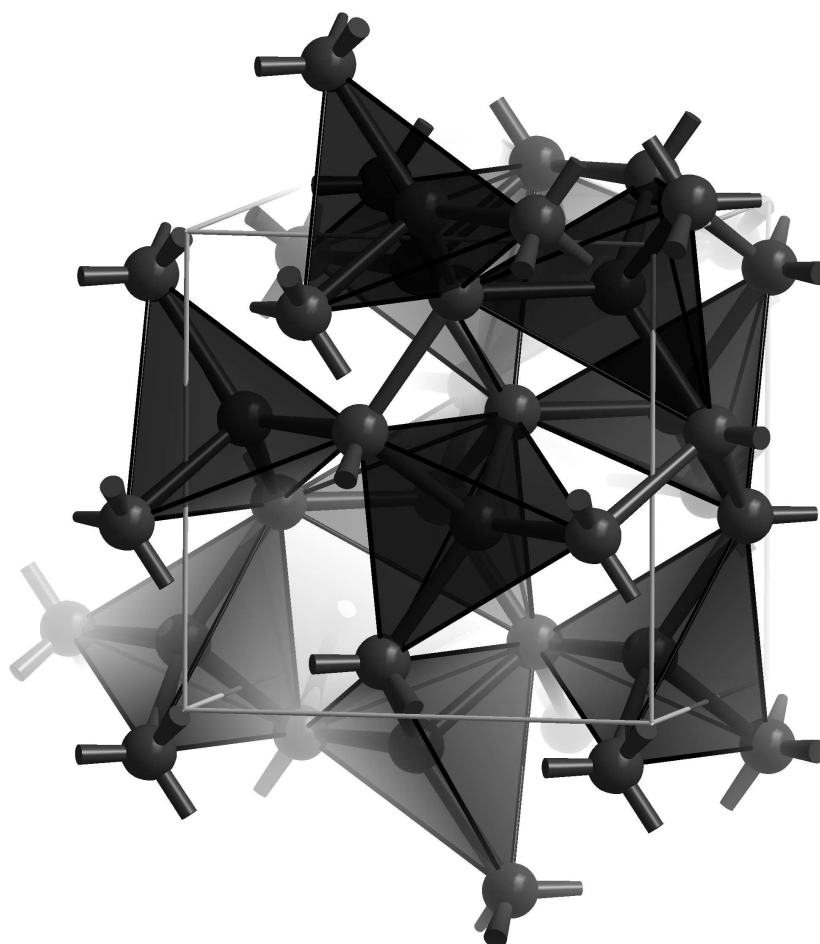


Fig. 1. Crystal structure of Si(cI16). Short interatomic distances $d(\text{Si-Si}) = 2.35 \pm 0.04 \text{ \AA}$ which are compatible with covalent single bonds are emphasized by dark lines. Distorted trigonal pyramidal coordination polyhedra are shaded. The cubic unit cell is indicated by thin grey lines.
624x624mm (96 x 96 DPI)

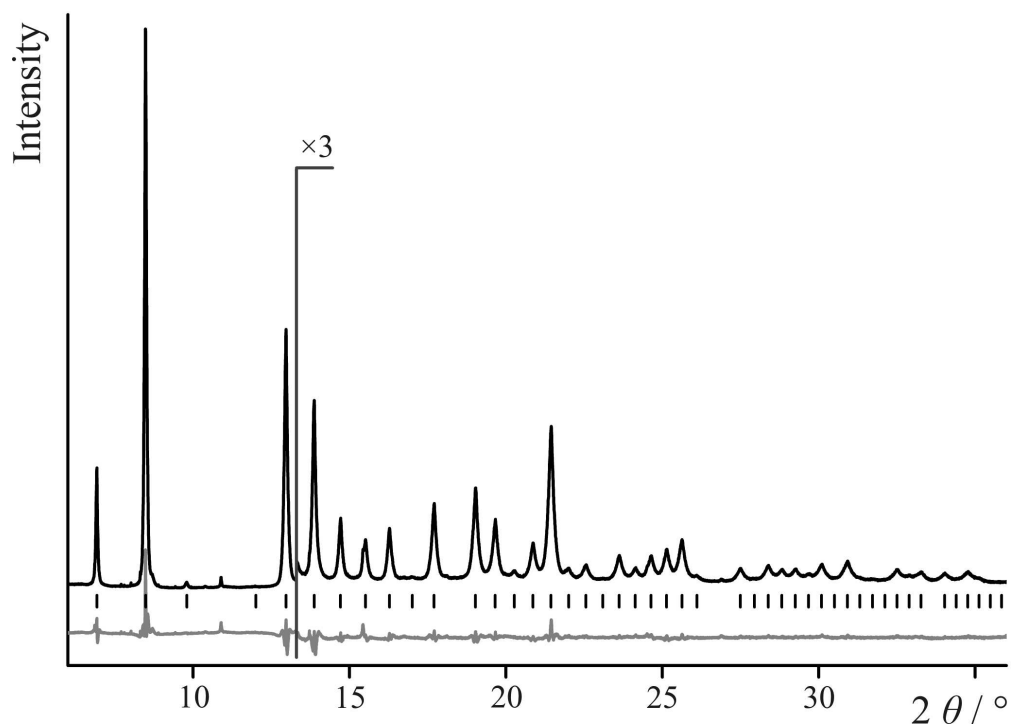


Fig. 2. X-ray powder diffraction diagram of Si(cI16) recorded using low-divergence synchrotron radiation at ID31 of the ESRF ($\lambda = 0.39987(2) \text{ \AA}$). The grey curve corresponds to the difference between observed and calculated intensities multiplied by a factor of three. Reflection positions are indicated by vertical bars.
87x62mm (600 x 600 DPI)

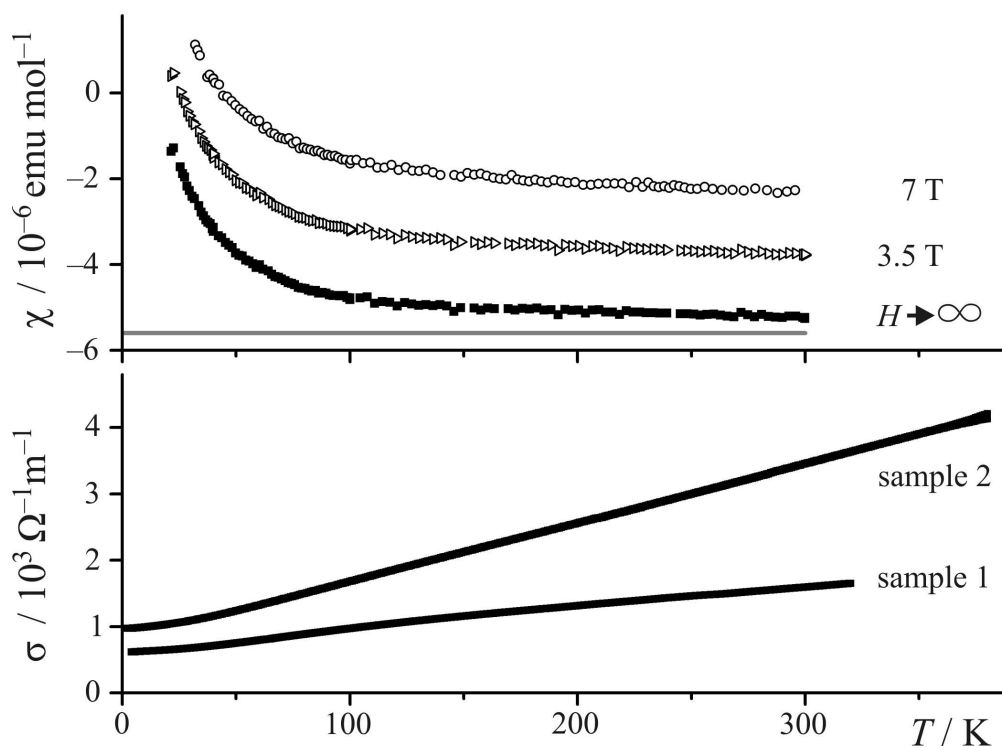


Fig. 3. Top: Measured ($\mu_0 H = 7.0 \text{ T}$ and 3.5 T) and extrapolated ($\mu_0 H \rightarrow \infty$) molar magnetic susceptibility $\chi(T, H)$ of the Si(cI16) sample. The grey line indicates the intrinsic temperature-independent term χ_0 for $T = 0 \text{ K}$. Bottom: Electrical conductivity $\sigma(T)$ of two Si(cI16) samples. The linear dependence above approximately 50 K is consistent with a heavily doped semiconductor.
88x65mm (600 x 600 DPI)

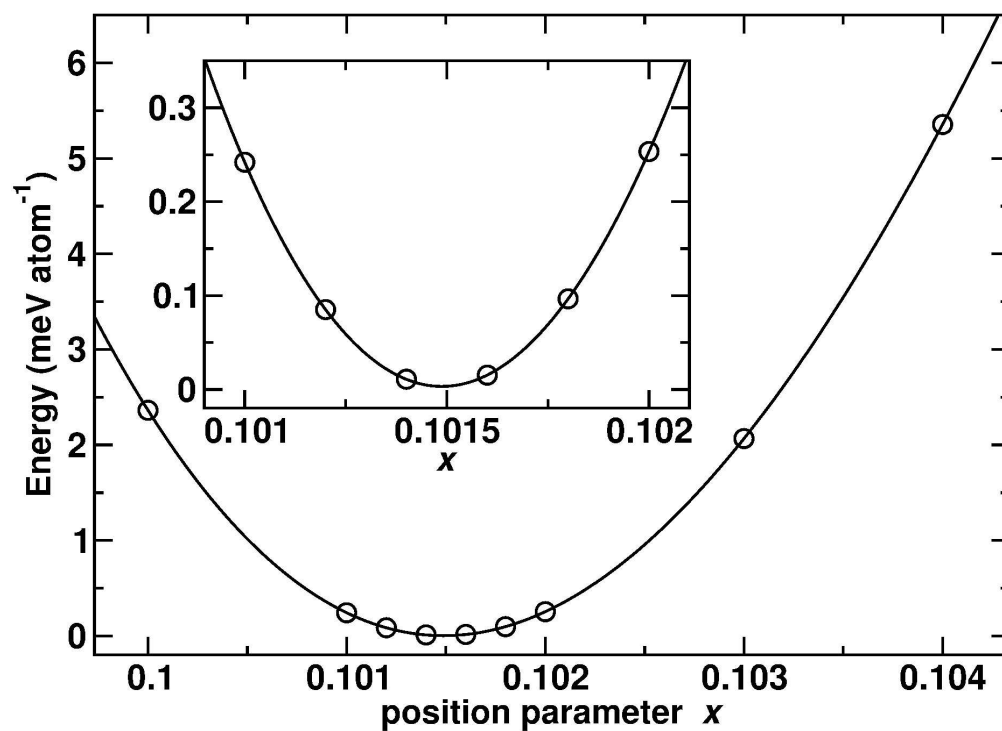


Fig. 4. Total energy as a function of the silicon coordinate. Open circles indicate calculated values, black lines represent a least squares fit of a fourth-order polynomial to the data. The minimum corresponds to $x = 0.10149(5)$ in perfect agreement with the experimental result. The insert shows an enlargement of the curve in the vicinity of the energy minimum.
236x170mm (600 x 600 DPI)

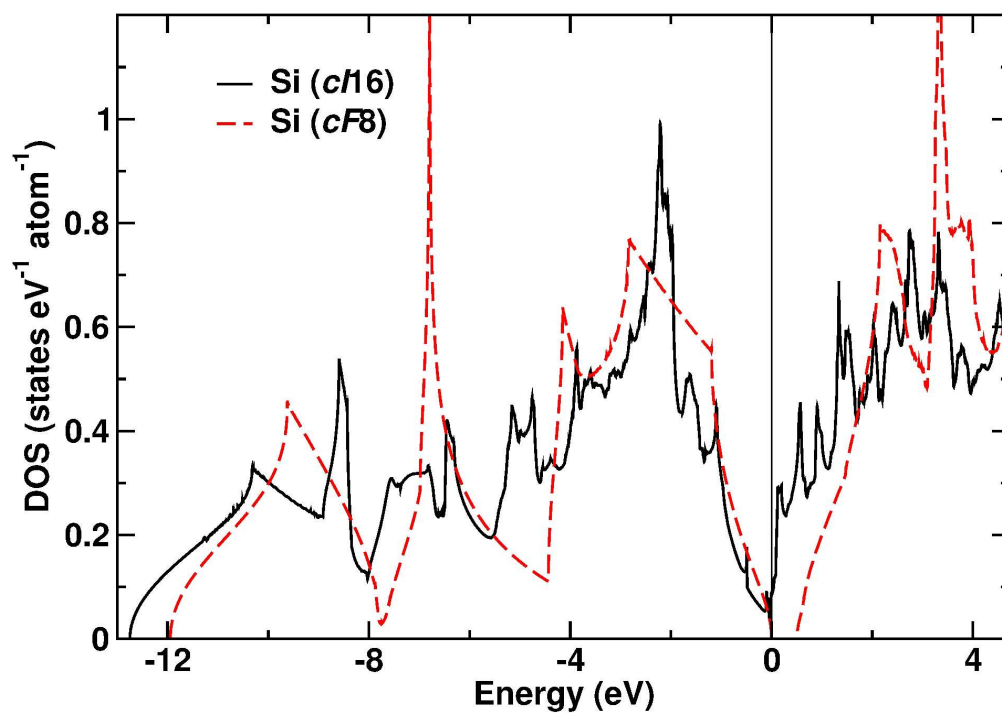


Fig. 5. Electronic density of states of Si(cF8) and Si(cI16). The LDA calculations reveal semiconducting behaviour for diamond-type silicon and a pseudo-gap with a low density of states for the metastable phase.
242x170mm (600 x 600 DPI)

Tab. 1. Details of the diffraction measurements and crystallographic data of Si(*c116*). Refinements are performed with the computer program WinCSD [27] Rietveld refinements are performed using Fullprof [28]. A Pseudo-Voigt function is used for profile simulation and a sixth order polynomial for modelling the background.

Compound	Si(<i>c116</i>)
Space group (No.)	<i>Ia</i> -3 (206)
Lattice parameters:	
Rietveld refinement of synchrotron data;	6.6265(1) Å;
Laboratory source with LaB ₆ standard;	6.6229(2) Å;
Earlier data	6.64(1) [7]
Unit cell volume / Å ³	290.97(1)
Refined position parameter Si(<i>x</i> , <i>x</i> , <i>x</i>)*;	0.10143(4);
Earlier data	0.103(1) [7]; 0.1025 [10]
$U_{11} = U_{22} = U_{33} = U_{iso} / \text{Å}^2$,	0.0058(2),
$U_{12} = U_{13} = U_{23} / \text{Å}^2$	0.0003(2)
Z	16
Calculated density / g cm ⁻³ ; Earlier data	2.564; 2.55 [7]
Diffractometer,	ESRF ID31,
wave length $\lambda / \text{Å}$	0.39987(2)
Diffraction set-up,	Transmission alignment,
Quartz capillary	<i>d</i> = 1 mm
Number of reflections,	97,
$2\theta_{max} / \text{Degree}$, step width / degree	36, 0.005
Residuals R_p ; R_{wp} ; R_{exp}	5.82; 7.84; 1.65
Interatomic distances with experimental	1 × 2.3283(4) Å; 2.369(9) Å [7]
errors as calculated in the full profile	3 × 2.3841(4) Å; 2.384(9) Å [7]
refinements *; Earlier data	1 × 3.4104(4) Å; 3.381(9) Å [7]
Angles / Degree; Earlier data	98.70(1); 98.1(3) [7]
	117.75(1); 118.0(4) [7]

* The maximal error of the internal coordinate as estimated on the basis of the number of observed reflections corresponds to 0.002.